International Journal of Nanomedicine

Dovepress
open access to scientific and medical research

Open Access Full Text Article

ORIGINAL RESEARCH

Activated Carbon nanoparticles Loaded with Metformin for Effective Against Hepatocellular Cancer Stem Cells

Lan Sun[1], Hong-Juan Yao[2], Jing-Cao Li[1], Bao-Quan Zhao[1], Yong-An Wang[1], Ying-Ge Zhang[1]

[1]Key Laboratory of Nanopharmacology and Nanotoxicology, Beijing Institute of Pharmacology and Toxicology, Beijing, People's Republic of China; [2]Key Laboratory of Antibiotic Bioengineering of National Health and Family Planning Commission (NHFPC), Institute of Medicinal Biotechnology (IMB), Chinese Academy of Medical Sciences and Peking Union Medical College (CAMS & PUMC), Beijing, People's Republic of China

Correspondence: Ying-Ge Zhang; Yong-An Wang, Beijing Institute of Pharmacology and Toxicology, Beijing, People's Republic of China, Tel +86 10-66930654; +86 10-66874607, Fax +86 10-68211656, Email Zhangyg58@126.com; yonganw@126.com

Introduction: Hepatocellular cancer stem cells (CSCs) play crucial roles in hepatocellular cancer initiation, development, relapse, and metastasis. Therefore, eradication of this cell population is a primary objective in hepatocellular cancer therapy. We prepared a nanodrug delivery system with activated carbon nanoparticles (ACNP) as carriers and metformin (MET) as drug (ACNP-MET), which was able to selectively eliminate hepatocellular CSCs and thereby increase the effects of MET on hepatocellular cancers.

Methods: ACNP were prepared by ball milling and deposition in distilled water. Suspension of ACNP and MET was mixed and the best ratio of ACNP and MET was determined based on the isothermal adsorption formula. Hepatocellular CSCs were identified as $CD133^+$ cells and cultured in serum-free medium. We investigated the effects of ACNP-MET on hepatocellular CSCs, including the inhibitory effects, the targeting efficiency, self-renewal capacity, and the sphere-forming capacity of hepatocellular CSCs. Next, we evaluated the therapeutic efficacy of ACNP-MET by using in vivo relapsed tumor models of hepatocellular CSCs.

Results: The ACNP have a similar size, a regular spherical shape and a smooth surface. The optimal ratio for adsorption was MET: ACNP=1:4. ACNP-MET could target and inhibit the proliferation of $CD133^+$ population and decrease mammosphere formation and renewal of $CD133^+$ population in vitro and in vivo.

Conclusion: These results not only suggest that nanodrug delivery system increased the effects of MET, but also shed light on the mechanisms of the therapeutic effects of MET and ACNP-MET on hepatocellular cancers. ACNP, as a good nano-carrier, could strengthen the effect of MET by carrying drugs to the micro-environment of hepatocellular CSCs.

Keywords: nanodrug delivery system, metformin, CD133, hepatocellular cancer stem cells

Introduction

Hepatocellular cancer is the third leading cause of cancer death worldwide and its incidence is increasing.[1–4] While better detection methods and treatment of hepatocellular cancer have improved disease outcomes at early stages, hepatocellular cancer remains largely incurable due to high recurrence rates and resistance to chemotherapy.[5,6] According to the cancer stem cell (CSC) hypothesis, CSCs, which are similar to normal adult stem cells, are at the germinal center of tumors, have the potential of differentiation and self-renewal.[7] Recently, increasing attention has been focused on better explanation of the initiation of relapse and metastasis in several types of carcinomas including hepatocellular cancers.[8,9] CSCs are able to differentiate into specific progeny which can initiate and maintain tumor growth.[10] It is believed that they could be a source for drug resistance, tumor recurrence, and metastasis.[11] These CSCs have been found in hepatocellular cancers with tumorigenicity and chemoresistance to CD133, which has been identified as an important marker of hepatocellular CSCs.[3] $CD133^+$ cells are proliferative, as evidenced by their high colony-forming efficiency.[12] Previous research demonstrated that $CD133^+$ cells originating from Huh-7 cells were more proliferative and possessed higher tumorigenic potential than their $CD133^-$ counterparts.[13] By immunohistochemistry, CD133 expression and elevated CD133 expression were associated with advanced tumor grade and elevated serum alpha-

Received: 5 August 2022
Accepted: 16 April 2023
Published: 31 May 2023

fetoprotein levels. In addition, patients with higher CD133 ratio in their tumors had shorter survival period and higher relapse rates compared with low CD133 patients. Multivariate analyses showed that increased CD133 expression was an independent prognostic factor for survival and tumor recurrence.[14] Therefore, the number of $CD133^+$ cells in hepatocellular cancer represents a key prognostic marker for hepatocellular cancer.

Metformin (MET), a traditional primary care drug for type II diabetes, is the most frequently prescribed hypoglycemic drug. Recently, the potential anticarcinogenic effects of MET were identified and have attracted increasing attention.[15–17] Notably, evidence was provided by recent research that MET holds promise for the efficient eradication of CSCs. It has been shown that low-dose MET combined with doxorubicin can selectively kill breast cancer stem cells and efficiently delay breast cancer relapse.[18,19] Some literature reported that MET could regulate breast cancer stem cell ontogeny by transcriptionally regulating the epithelial–mesenchymal transition state associated with CSC-related cellular phenotypes.[20] The works of Bao et al showed that MET inhibits pancreatic CSCs' growth by modulating miRNA expression.[21] Due to the difficulty of studying in vivo quantity relation between CSCs and tumor size, there has been scarce literature reporting the in vivo effects of MET on CSCs.

Nanosized activated carbon particles with spherical morphology, relatively smooth surfaces, stronger absorption, better lymph taxis, high rate of cell-uptake,[22,23] and excellent targeting effects of cancer have been used as tracer of drainage lymph node to assist with section surgery of stomach cancers and drug carriers.[24] When intra-peritoneally injected, activated carbon nanoparticles (ACNP) as drug carriers can improve the drug concentration in the abdomen cavity, peritoneal tissues and abdominal drainage lymph canal that can be accurately measured and calculated by mathematical equations.[25,26] Because of the slow-release of ACNP for the drugs, the drug concentration in peritoneal and lymph tissues can be maintained for a much longer time than free drugs.[27] At the same time, ACNP-based drug delivery systems can decrease the drug concentration in blood and thereby decrease the drug's toxicity.[24,28–31] Through increasing the drug concentration in therapy-related tissues, ACNP can improve the therapeutic effects of anticancer drugs significantly.

To find more effective chemotherapy for hepatocellular cancers, we prepared a nanodrug delivery system with ACNP as carriers and MET as drug (ACNP-MET). The in vitro and in vivo effects of ACNP-MET on hepatocellular cancers were investigated, paying special attention to the effects of MET and ACNP-MET on CSCs.

Materials and Methods

Materials

Metformin hydrochloride (MET) was obtained from Sigma-Aldrich, USA. Dulbecco's Modified Eagle Medium (DMEM) was purchased from Hyclone, USA. Fetal bovine serum (FBS), B27 supplement, TrypLE and EDTA were purchased from Gibco, USA. Epidermal growth factor (EGF), basic fibroblast growth factor (bFGF), Human anti-CD133/2(293C3)-PE and its isotope were obtained from MiltenyiBiotec, USA. Cell Counting Kit-8 (CCK-8) was purchased from Dojindo Molecular Technologies, Japan. Apoptosis kit was purchased from Becton, Dickinson and Company, USA. Phosphate-buffered saline (PBS), penicillin and streptomycin were purchased from North China Pharmaceutical, People's Republic of China. Human Huh-7 cell (HHC) line was obtained from the Beijing Cell Bank of the Chinese Academy of Medical Sciences, People's Republic of China. Ultralow attachment six-well plates were purchased from Corning, USA.

Preparation of Activated Carbon Nanoparticles (ACNP)

ACNP with uniform diameters and form were prepared with a ball-milling-precipitation method. The market activated carbon particles were grounded using pulverisette 7 planetary micro mill to obtain a mixture of activated carbon particles with various diameters. These activated carbon particle mixtures were suspended in triple distilled water in a concentration of 200 g/100L under stirring. The prepared suspension (S1) was allowed to stand still for 7 days. These particles would participate in an order from larger to smaller depending on the difference of sedimentation coefficient. After 7 days, the suspension in the top 10 cm was taken out and was filtrated with a filter with certain diameter pores. The particles which accumulated on the filter that could not leach through the pores were collected, and were then re-suspended in triple-distilled water (S2). Packaged into 15 mL glass ampoules, S2 was placed in a −80°C refrigerator for freeze drying. A kind of black powder composed of ACNP was obtained after 24 h freeze-drying. For ACNP characterization, the particles of the

powder were re-suspended in triple-distilled water again (S3), which was dropped onto copper mesh for transmission electron microscope (TEM, Hitachi H7650, Hitachi Ltd., Tokyo, Japan) or onto fresh mica surface for atomic force microscope (AFM, JPK NanoWizard I, Germany) morphology observation. Under AFM, the ACNP diameter was measured with JPKSPM Data Processing software (JPK, Berlin, Germany) and was measured with a metallography image analyzer (AMT V600 software, Advanced Microscopy Techniques, MA, US) under TEM. And the hydrodynamic diameter and Zeta potential of nanoparticles were examined through dynamic light scattering (DLS) in a Zetasizer Nano ZS (Malvern, UK).

The Preparation of ACNP-MET Drug Delivery System (ACNP-MET)

MET solubilized in PBS was stored at −20°C and used within 2 weeks.

ACNP suspension and MET solution were blended in a certain proportion of concentrations. The mixture was placed in an ultrasound field (40 Hz, 300 W) for 4 hours to allow MET to sufficiently enter the micropores of ACNP and was then allowed to stand still for 20 minutes. The adsorption of MET on ACNP was achieved by the self-assembling of MET on the surface of the micropores of ACNP at a temperature of 0°C. The quantity of MET absorbed on ACNP was detected by measuring the concentration of MET in the suspension(C). At different time, 1 mL suspension was withdrawn and centrifuged. The absorbance at 233 nm of the supernatant of centrifugation was detected in a UV-spectrophotometer. The concentration of MET was calculated from the absorbance-concentration standard curve. The drug loading (Q) was calculated with formula $Q=(Q_0\text{-}VC)/M$, where Q_0, V and M were respectively the added quantity of MET, the volume of the supernatant and the mass of added ACNP. Changing proportions of ACNP to MET, the best adsorption can be achieved (Q_m). The best ratio of ACNP and MET was determined based on the isothermal adsorption formula $C/Q=1/K*Q_m+C/Q_m$. $Q_m$was the maximum quantity of MET loaded by ACNP.

Determination of the MET Release Rate of the ACNP-MET Drug Delivery System (ACNP-MET)

To test the MET release rate, 5 mg ACNP-MET was dispersed in 5 mL PBS (PH=7.4) and transferred into disposable cut-off dialysis bags (MWCO 1000 Da) which were sealed and then immersed in 40 mL of release medium with shaking at 100 rpm at 37°C. A volume of 1 mL release medium was taken at predetermined time intervals, followed by immediately replenishing the equal volume of fresh medium. The concentration of released MET in release medium was determined by UV-visible spectroscopy, and the amount of released MET was calculated using the formula: W=VC where V was the volume of release medium and C was the concentration of MET in release medium. The cumulative released rate (RR, %) was calculated using the formula: RR%=Wi/Wt×100% where Wi is the measured amount of MET in the release medium at the given time point, and W_t is the total amount of MET in the equal volume of ACNP suspensions before dialysis. Each experiment was repeated three times.[29,32]

Cell Culture and Hepatocellular Cancer Stem Cells (CSCs) Sorting

Human Huh-7 cell (Huh-7) line was cultured in DMEM with 10% FBS at 37°C in 95% O_2 and 5% CO_2. The control and the experimental groups were cultured under the same conditions.

Using anti-CD133/2(293C3)-PE antibodies, hepatocellular CSCs were sorted from Huh-7 cells by a flow cytometry instrument (BD FACSAria, USA). Next, the sorted $CD133^+$ cells were seeded in ultra low attachment six-well plates and cultured in stem cell medium (DMEM, 1% B27 supplement, 10 μg/mL bFGF, 20 μg/mL EGF, 100 U/mL penicillin, and 100 μg/mL streptomycin) at 5% CO_2 and at 37°C. In this circumstance, Huh-7 CSCs grew into nonadherent spherical clusters, also known as mammospheres which were further harvested by centrifugation at 1000 rpm for 5 min and planted in the same medium at 1×10^4 cells/mL.[33]

Identification of Hepatocellular Cancer Stem Cells (CSCs)

The mammospheres were collected and digested by 0.25% trypsin solution. Then separated single cells were washed with cold PBS (pH=7.4) and stained by anti-CD133-PE at 4°C in the staining buffer or with isotype control staining. After 30 min, this sample was washed 3 times with cold PBS, and resuspended to a final volume of 5 mL with PBS to be analyzed by FACSAria.[33]

Inhibition of the Proliferation of Hepatocellular Cancer Stem Cells (CSCs)

CCK-8 assay was used to assess the inhibitory effect of drugs on the hepatocellular CSCs. These cells were sorted from Huh-7 cells and seeded into 96-well culture plates at 5000 cells/well. And then, they were incubated at 37°C in a humidified atmosphere of 95% O_2 and 5% CO_2. After 24 h, the cells were exposed to a range of concentrations of MET, ACNP or ACNP-MET, respectively. The final concentration of ACNP-MET and MET were 200 ~ 1600 and 50 ~ 400 μg/mL, respectively. The concentration of ACNP-MET was calculated in the concentration of MET. Normal saline was used as blank control and free MET was used as positive control. After the addition of these drugs, the cells were further cultivated for 48 hours. The proliferative activity was measured by the CCK-8 assay and the absorbance measurement was made by microplate reader (Thermo Fisher Scientific, USA) at 450 nm.[34] The inhibition rate was calculated with the following formula: inhibition rate (%)=(the absorbance value for the control cells-the absorbance value for the treated cells/the absorbance value for the control cells) ×100%. The dose-effect curves were obtained when the experiments were performed three times independently.

Inhibition of the Self-Renewal Capacity of Hepatocellular Cancer Stem Cells (CSCs)

$CD133^+$ Population Assay

To measure the effects of drugs on CD133 expression, Huh-7 cells were suspended in complete medium (DMEM containing 2% FBS) and seeded into culture bottle. These cells were cultured at 37°C for 24 h in 5% CO_2 incubator. These cells were then exposed to MET, ACNP and ACNP-MET, diluted in complete medium at 1.0 mM for 72 h. The blank medium was used as a control. After the 72 h treatment, cells were harvested, washed with PBS, and resuspended in complete medium. The density of cells was 1×10^6 cells/mL. Then, anti-CD133/2(293C3)-PE or its isotype control were added to the cell suspension and incubated at 4°C in the dark for 30 minutes. Treated cells were washed with wash buffer and then fixed with 1% paraformaldehyde in PBS, followed by analyzing with BD FACScalibur (BD Biosciences, USA) within 1 h.

Mammosphere Formation Inhibition Assay

Mammosphere culture was performed as previously described.[35,36] $CD133^+$ and $CD133^-$ cells were isolated by flow cytometry and seeded in six-well ultra low attachment plates at 2000 cells/well. Cells were grown in serum-free F-12/DMEM containing 0.02 μg/mL, 20 ng/mL EGF and 2% B27. Cultures were maintained at 37°C in a humidified atmosphere of 5% CO_2 for 24 h. Then, cells were treated with MET, ACNP and ACNP-MET, respectively. After being cultured for 7 days, tumor sphere counts and diameter measurement were performed. The percentage mammosphere-forming efficiency (MSFE) was calculated according to the following equation: MSFE= (number of spheres-like structures (large diameter>50 μm)/ number of cells initially seeded) ×100%.[19,37,38]

In vivo effects on the Tumor Model Formed by Hepatocellular Cancer Huh-7 Cell Xenografts

The tumor model was established by xenografting Huh-7 cells into non-obese diabetic/severe combined immunodeficiency (NOD/SCID) mice. Four-week-old NOD/SCID mice were obtained from Experimental Animal Center of Beijing Academy of Medical Sciences (Beijing, People's Republic of China). NOD/SCID mice were maintained in accordance with guidelines established by the Committee on Animals of Beijing Academy of Medical Sciences and housed in a specific pathogen-free facility. All animal experiments followed the principles of the National Institutes of Health Guide for the Care and Use of Laboratory Animals. All procedures were approved by the Institutional Animal Care and Use Committee of Beijing Academy of Medical Sciences.

NOD/SCID mice were randomly divided into two groups, namely, control group and treated group (N=5 mice). 3×10^6 Huh-7 cells were subcutaneously injected into the left flanks of NOD/SCID mice. When the tumors reached 100–150 mm^3 in volume, the mice were treated with MET, ACNP and ACNP-MET once per 4 days i.v. at 150 mg/kg. The total frequency was four. The control group received vehicle only (100 μL, 0.9% NaCl). The NOD/SCID mice were monitored daily for tumor progression. Tumor volume (V) was calculated with the following formula: V= (length×width^2)/2 (mm^3). 26 days later, NOD/SCID mice were sacrificed and the tumors were collected.[39]

For investigation of the fraction of CSCs in the tumors, freshly excised tumor samples were immediately mechanically homogenized, enzymatic-dissociated and filtered.[37] The harvested cells were washed and resuspended at 1×10^6 cells/mL in PBS, then $CD133^+$ cell analysis was performed as described previously. Through $CD133^+$ cell analysis, the percentage of $CD133^+$ cells in tumor was obtained, which was noted as P_{+}. Correspondingly, the percentage of $CD133^-$ cells in tumor was P-=1-P_{+}. Thus, the tumor volume (V) is the sum of $CD133^+$ cell volume (V_{+}) and $CD133^-$ cell volume (V-). Taking the control tumor volume as V_0 and the drug treated tumor volume as V_I, the volume inhibition rate (I_V) can be calculated with formula $I_V=(V_0-V_I)/V_0\times100\%$. Taking the measured percentage of $CD133^+$ cells in control tumor as P_{0+} and that in treated tumor as P_{I+}, the volume of $CD133^+$ cells in control tumor and treated tumor are respectively $V_{0+}=V_0P_{0+}$ and $V_{I+}=V_IP_{I+}$. Correspondingly, the volume of $CD133^-$ cells in control tumor and treated tumor are respectively $V_{0-}=V_0P_{0-}$ and $V_{I-}=V_IP_{I-}$. The inhibition rate of drugs on CSCs cells in vivo (I_{CSC}) can be calculated from V_{0+} and V_{I+} in formula $I_{CSC}=(V_{0+}-V_{I+})/V_{0+}$. The corresponding inhibition rate of drugs on common cancer cells (I_{CCC}) can be calculated with formula $I_{CCC}=(V_{0-}-V_{I-})/V_{0-}$, where $V_{0-}=V_0-V_{0+}$ and $V_{I-}=V_I-V_{I+}$.

Statistical Analysis

Data are presented as the mean ± standard deviation. One-way and two-way ANOVA were used to decide significant differences among groups. LSD was used to analyze all experimental data. P-values < 0.05 were considered statistically significant. All statistical analysis was performed using SPSS 16.0 software.

Results

Activated Carbon Nanoparticles (ACNP) and ACNP-MET Drug Delivery System (ACNP-MET)

The AFM and TEM images showed that the ACNP prepared by the ball-milling-precipitation method has regular morphology, with uniform particle size, smoother surface and approximate globular shape as shown in Figure 1A and B. Under AFM, the ACNP diameter was measured with JPKSPM Data Processing software (JPK, Berlin, Germany), the average ACNP size was 74.05±14.01 nm. Under TEM, the ACNP diameter was 63.60±15.27 nm with a metallography image analyzer (AMT V600 software, Advanced Microscopy Techniques, MA, US). The average particle size was 188 nm as measured by laser particle size analyzer (Figure 1C). The Zeta potential was determined by dynamic light scattering (DLS) in a Zetasizer Nano ZS (Malvern, UK). The zeta potential measurements of ACNP and ACNP-MET were −21.6±1.1 mV and −14.1±0.1 mV respectively.

In the concentration range of 1~10 μg/mL, the absorbance (A) of MET has a linear positive correlation with the concentration (C) of MET, and the linear regression equation is written in the form of : A=0.00479+0.08137C (r^2=0.9995, P<0.0001) (Figure 2A). At 20°C, the adsorption of ACNP for MET reached the equilibrium state within about 4 h (Figure 2B). The adsorption isotherm equation was C/Q= −0.00531+0.00399C (r^2=0.995, P<0.001) and the saturated adsorption quantity of ACNP for MET: Qm=256.17 mg/g at mass ratio of ACNP: MET=4:1 (Figure 2C).

Figure 2D shows the in vitro release profiles of MET from ACNP-MET at 37°C in PBS buffer. The release ratio of MET was 20.69% during 72 h.

Sorting and Identification of Hepatocellular Cancer Stem Cells (CSCs)

It was reported that $CD133^+$ hepatocellular cancer cells have the characteristics of hepatocellular cancer stem cells. We used fluorescence-activated cell sorting (FACS) method to isolate $CD133^+$ cells from Huh-7 cells because CD133 serves

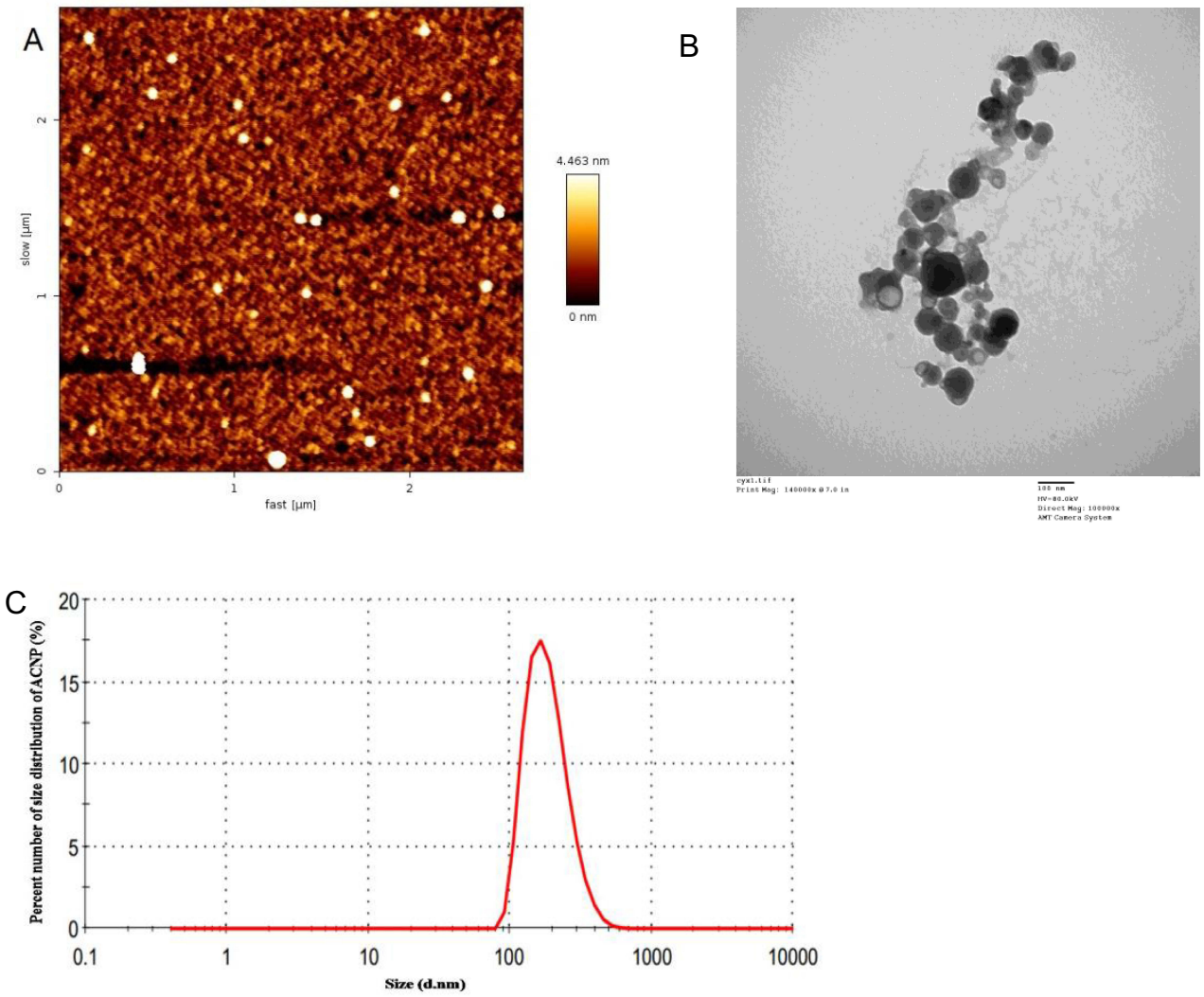

Figure 1 Characterization of ACNP. (**A**) AFM image of ACNP. (**B**) TEM image of ACNP. (**C**) size distribution of ACNP by laser particle size analyzer.
Notes: Adapted from Sun L, Cai Y, Liu Y, Song D, Liu Y, Yao H, Zhang Y. Activated Carbon Nanoparticles As Carriers of Anticancer Drugs. Nano Biomed. Eng. 2013, 5(2), 94-101.(A,B) 2013 S. Lan et al. Creative Commons Attribution License.[24]

as a marker of CSCs in hepatocellular cancer. The results showed that the ratio of $CD133^+$ cells in hepatocellular cancer Huh-7 cells was 6.08±0.80% (Figure 3A).

In order to assess the self-renewal potential of the $CD133^+$ cells, we employed tumor sphere culture to explore the $CD133^+$ subset cells that produced spheroid colonies. These isolated $CD133^+$ and $CD133^-$ cells were cultured in serum-free media. After 7 days, we found that there were some spheroid colonies from $CD133^+$ cells in serum-free media under non-adherent conditions (Figure 3B, b1), while $CD133^-$ cells formed few or no colonies (Figure 3B, b2), which indicated that $CD133^+$ hepatocellular cancer Huh-7 cells could be used as a model of hepatocellular cancer stem cells. After flow sorting and culture, the proportion of $CD133^+$ cells could reach 92.81±0.22% (Figure 3C).

Inhibition of the Proliferation of Hepatocellular Cancer Stem Cells (CSCs)

The CCK-8 assay showed the inhibitory effect of MET and ACNP-MET on $CD133^+$ and $CD133^-$ cells for 48 h (Figure 4). The IC50 values of MET and ACNP-MET on $CD133^+$ cells were 54.51 µg/mL and 2.85 µg/mL, respectively. In addition, the IC50 values of MET and ACNP-MET on $CD133^-$ cells were 25.14 mg/mL and 317.00 µg/mL, respectively. Both MET and ACNP-MET displayed stronger inhibitory effects on the $CD133^+$ cells than that on the $CD133^-$ cells, which indicated that hepatocellular CSCs were more sensitive in suppression to MET than

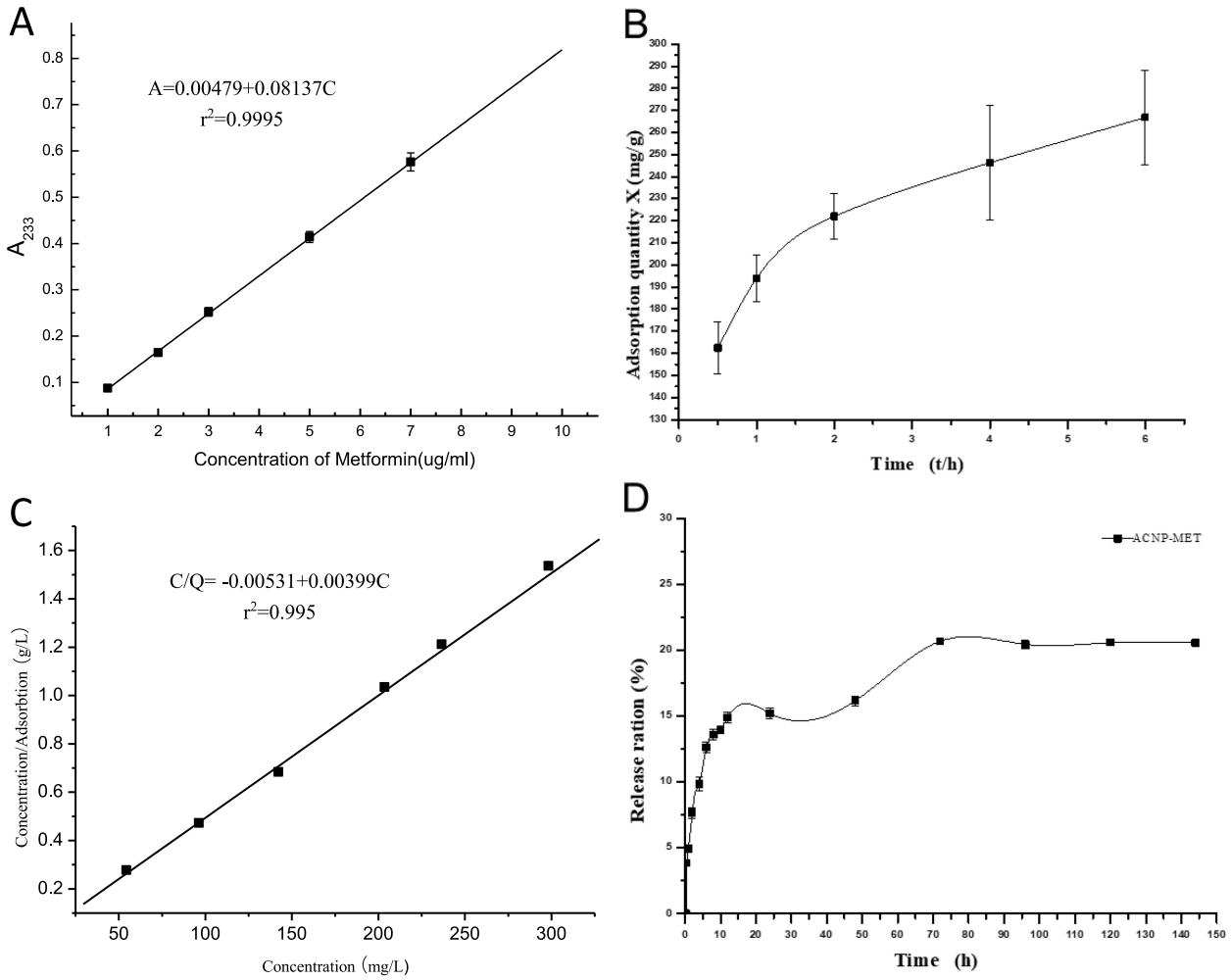

Figure 2 Drug loading of ACNP-MET. (**A**) Standard curve. A=0.00479+0.08137C (r^2=0.9995, P<0.0001). (**B**) adsorption-time relation. (**C**) adsorption-concentration curve. C/Q= −0.00531+0.00399C (r^2=0.995, P<0.001), C is the concentration of MET in the suspension, Q is the drug loading; saturated adsorption quantity of ACNP for MET: Qm=256.17 mg/g at mass ratio of ACNP: MET=4:1. (**D**) A release profile of MET from ACNP-MET in PBS buffer at 37°C. The release rate of MET was 20.69% during 72 h. Data are presented as the mean±standard deviation (SD).

hepatocellular cancer cells. ACNP-MET had inhibitory effects significantly stronger than MET on both the $CD133^+$ and $CD133^-$ cells. ACNP did not show any toxicity on the $CD133^+$ cells and $CD133^-$ cells even at the highest concentration, suggesting that ACNP can be used as a drug delivery vehicle without serious cytotoxicity. From the results shown in Figure 4, it can be concluded that ACNP as the carrier of MET increases the inhibition effects of MET on both CSCs and hepatocellular Huh-7 cells.

Inhibition of the Self-Renewal Capacity of Hepatocellular Cancer Stem Cells (CSCs) in vitro

In Figure 5A and B, the effects of MET and ACNP-MET on the percentage of Huh-7 cells expressing the hepatocellular CSCs marker CD133 were shown. A dose-dependent effect of $CD133^+$ subpopulation was clearly shown when Huh-7 cells were treated with graded concentration of MET and ACNP-MET. After the cells were treated at 200 μg/mL for 72 h, the proportion of $CD133^+$ cells in ACNP group was 4.48±0.16%, whereas the proportion of $CD133^+$ cells was obviously decreased to 2.65 ±0.45% and 0.43±0.07% in MET and ACNP-MET treated groups respectively. This result indicates that ACNP-MET

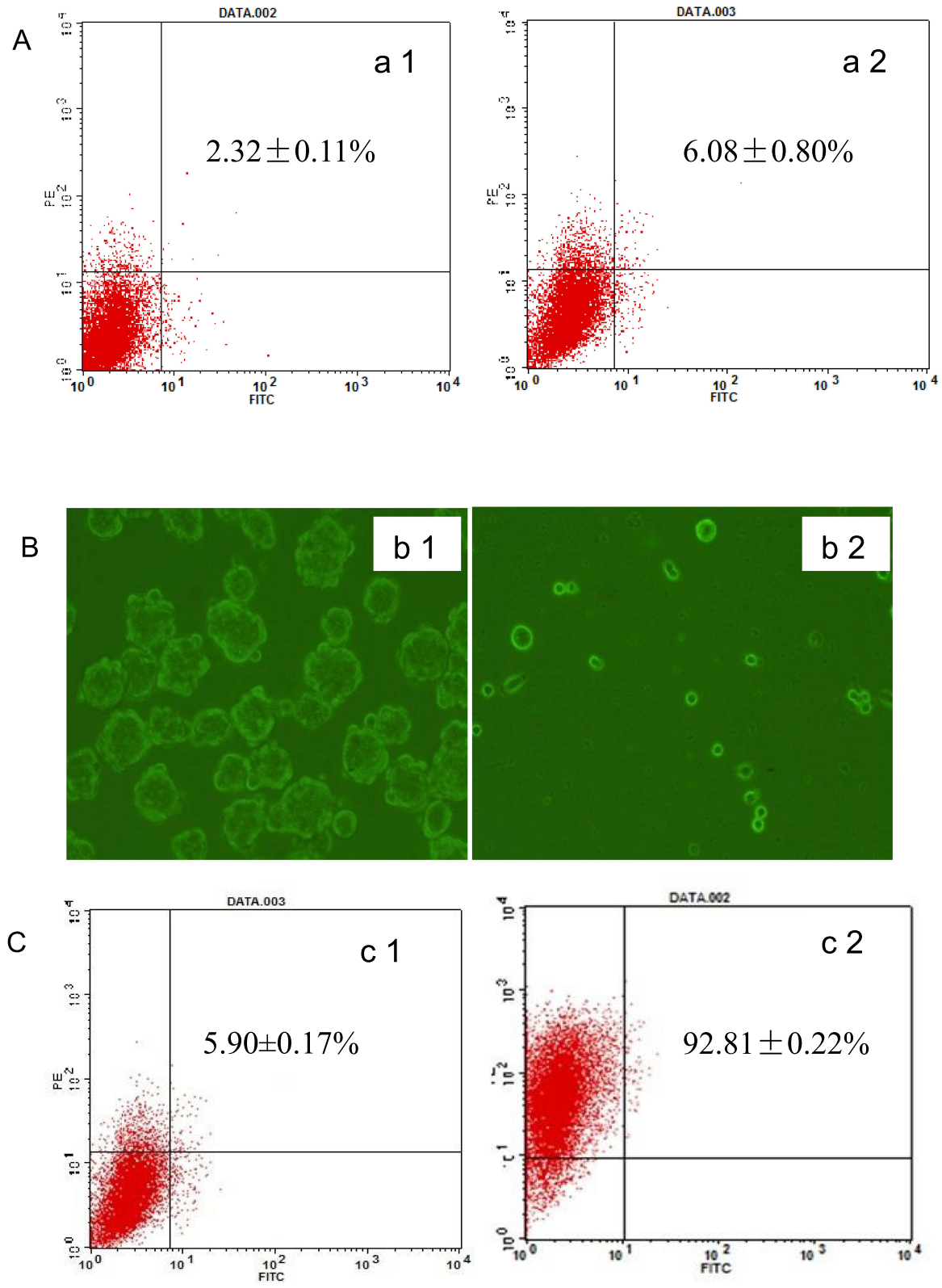

Figure 3 Sorting of hepatocellular CSCs. (**A**) Expression of CD133 marker in hepatocellular cancer line Huh-7 by fluorescence-activated cell sorting (FACS) analysis. (**a1**) CSCs stained with IgG-PE antibody as isotype control; (**a2**) CSCs stained with anti-CD133-PE antibody. (**B**) Image of $CD133^{+}$ cells (**b1**) and $CD133^{-}$ cells (**b2**) sorted from Huh-7 cells cultured in serum-free medium for 7 days under the light microscope. (**C**) Identification of the phenotype of the hepatocellular CSCs cultured for 7 days in serum-free medium. (**c1**) CSCs stained with IgG-PE antibody as isotype control; (**c2**) CSCs stained with anti-CD 133-PE antibody.

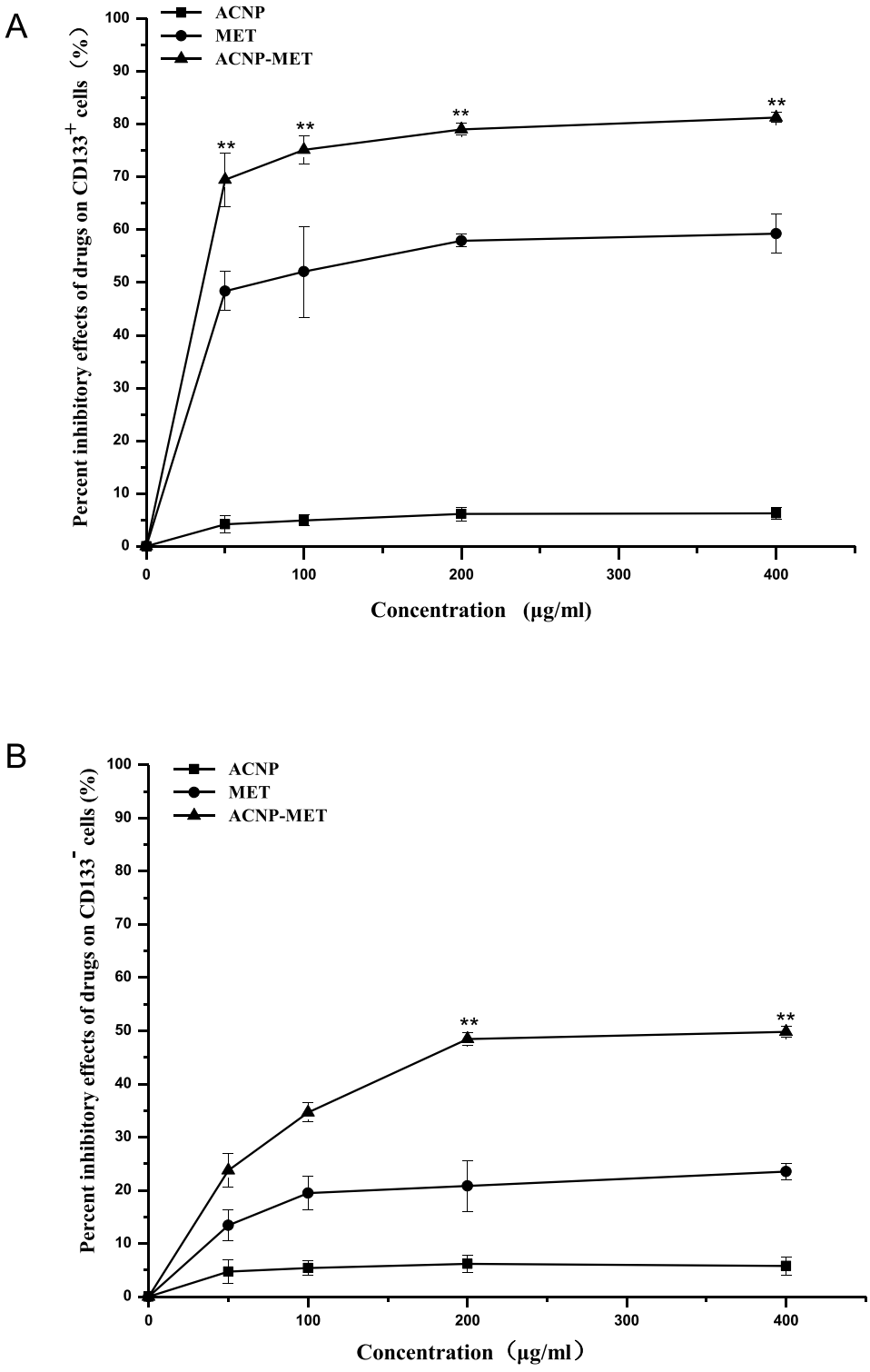

Figure 4 Inhibitory effects of drugs on $CD133^+$ cells (**A**) and $CD133^-$ cells (**B**) at 48 h measured by CCK-8 assay after treatment. Data are presented as mean ± SD from triple experiments. **P < 0.01, versus free MET.

exhibited the strongest selectively toxicity to hepatocellular CSCs, resulting in proportion of $CD133^+$ cells decrease, which suggests MET and ACNP-MET may inhibit hepatocellular cancer through their preferential effects on CSCs.

Mammosphere formation assay was a standard and a very important approach to characterize stem cell-like properties in vitro.[37,40] According to the current theory of CSCs, the scientists believe that noncancer stem cells will die if they are

placed in serum-free medium and suspension culture.[40,41] And they had confirmed that mammospheres are enriched in cells with functional characteristics of stem cells.[33] The formation of mammospheres is directly proportional to the number of self-renewing stem cells, which is sufficient to evaluate the effect of treatment on stem cells.[37,42,43]

Figure 5C shows the ability of $CD133^+$ cells to form mammospheres when they were treated with ACNP and ACNP-MET at different concentrations. Under light microscope, the capacity of $CD133^+$ cells forming mammospheres treated with blank ACNP (Figure 5C-b) was conserved as the same as control (Figure 5C-a).

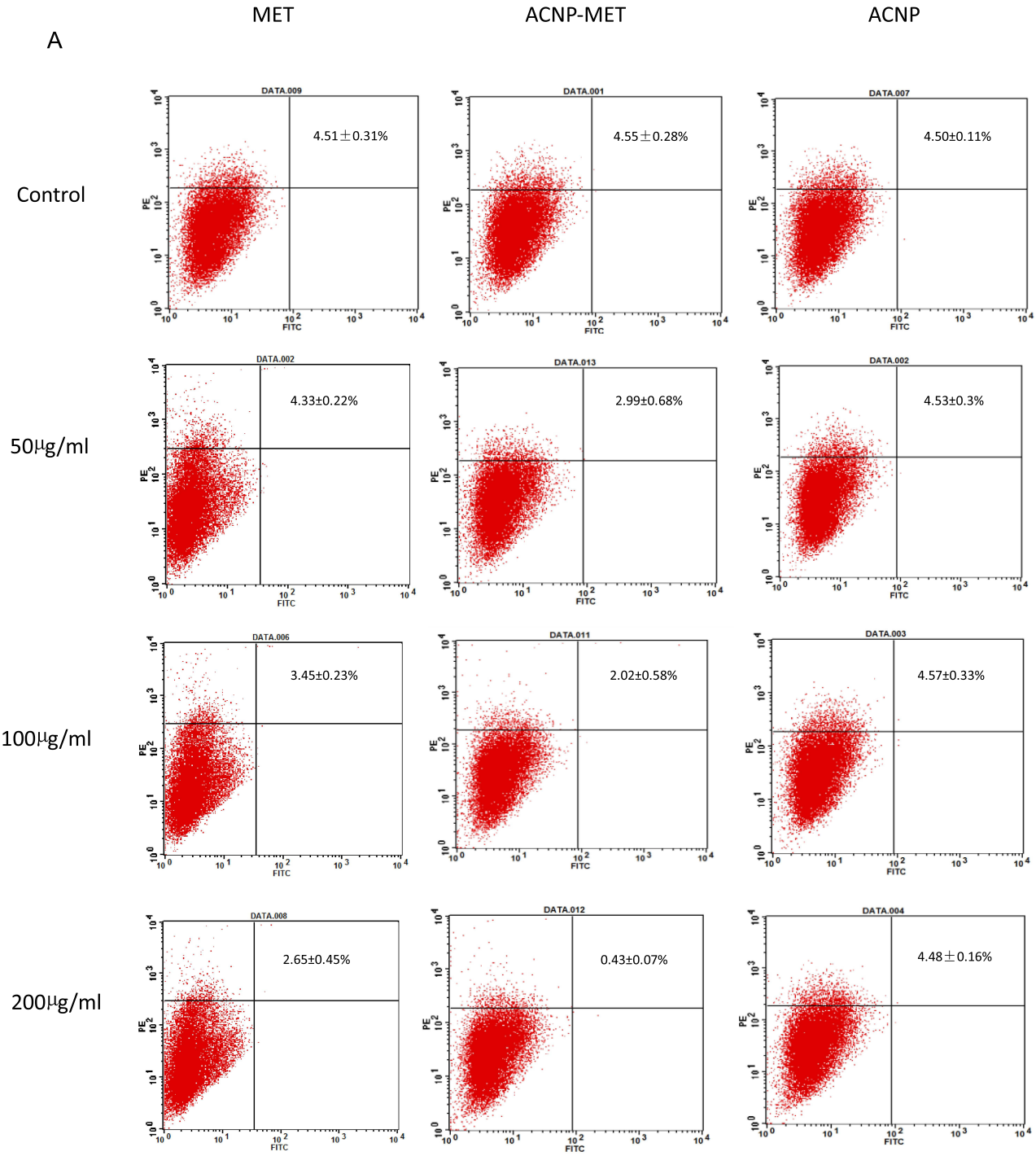

Figure 5 Continued.

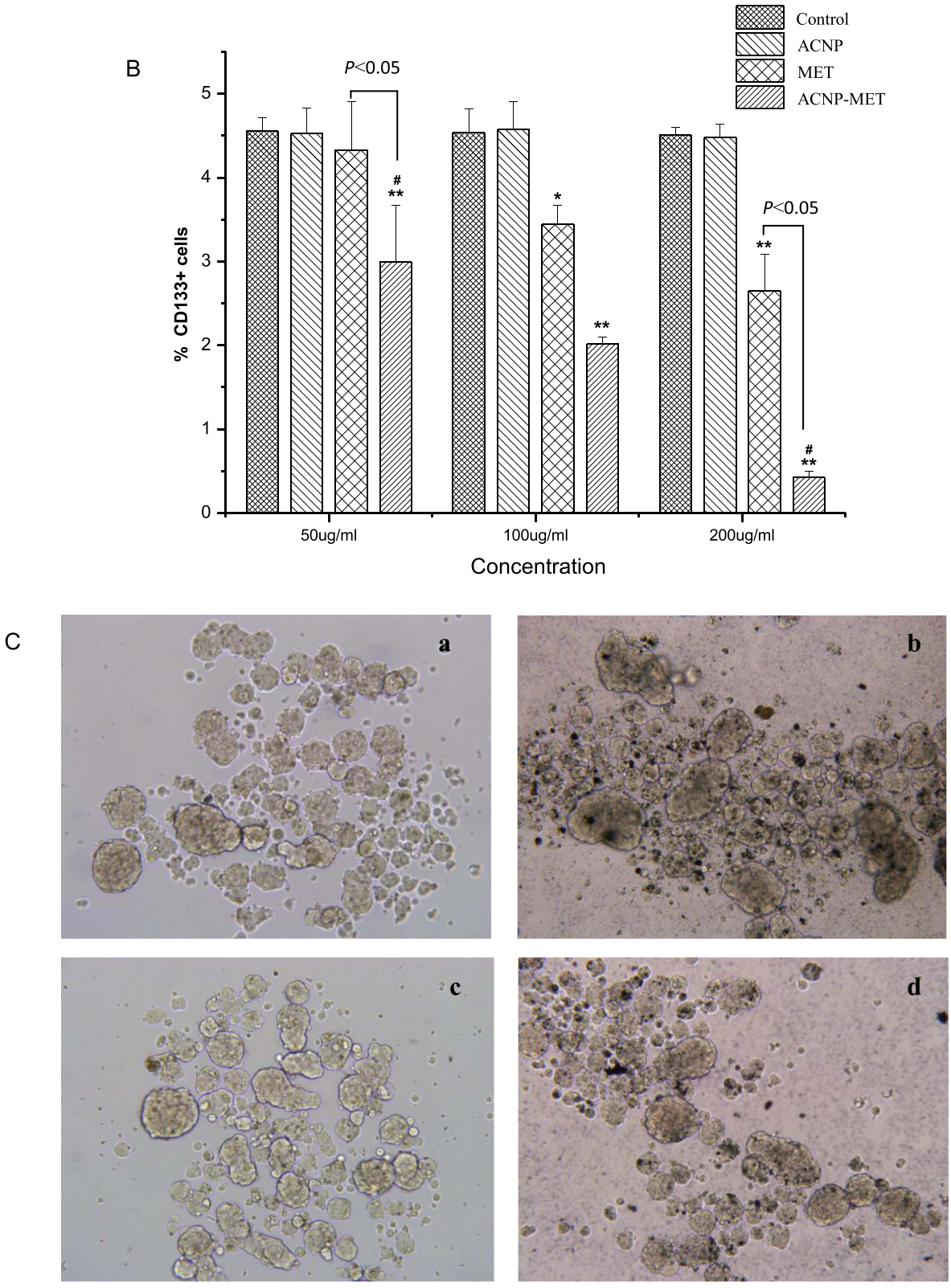

Figure 5 Continued.

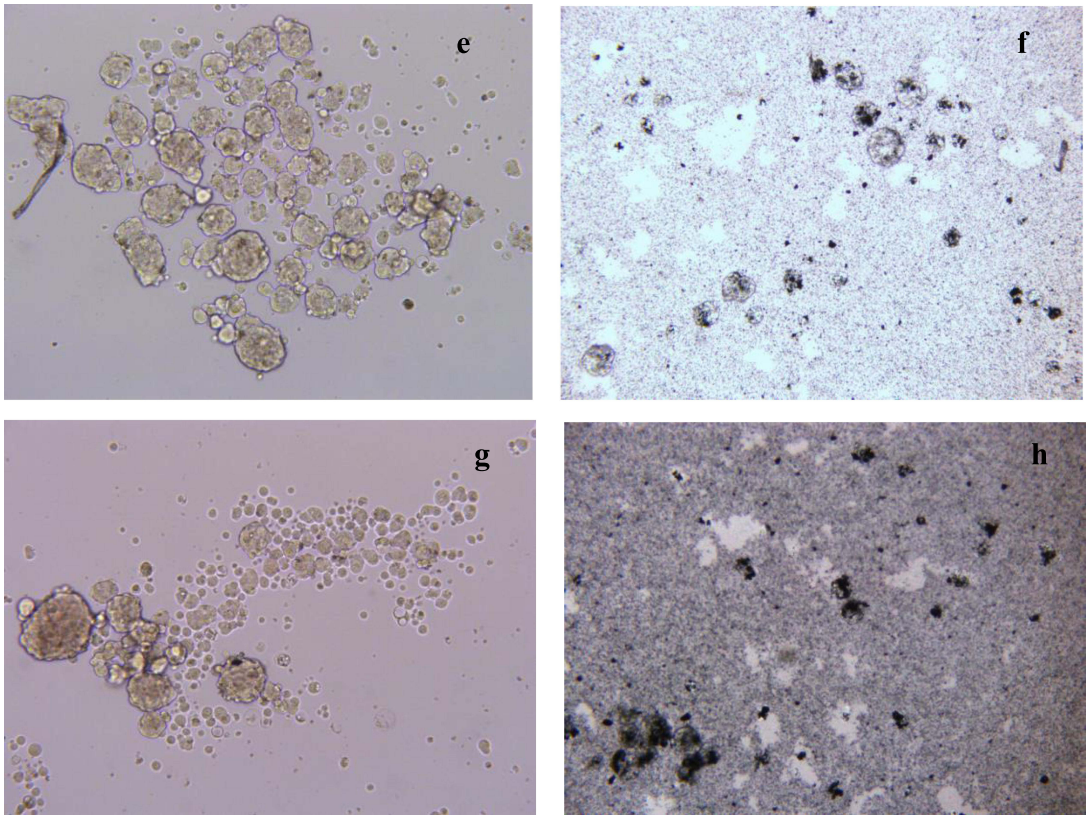

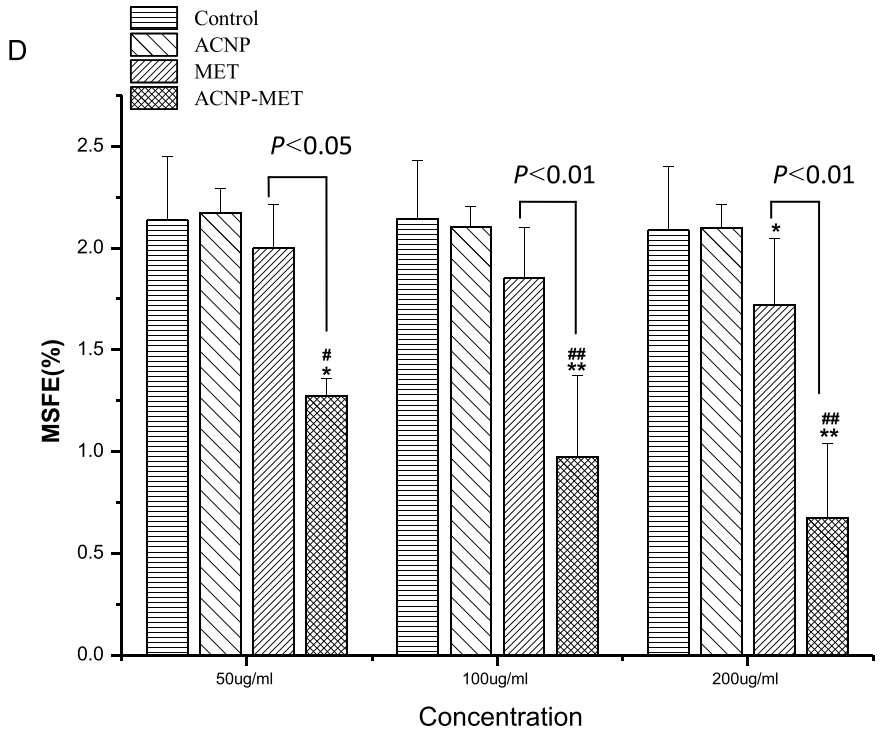

Figure 5 Continued.

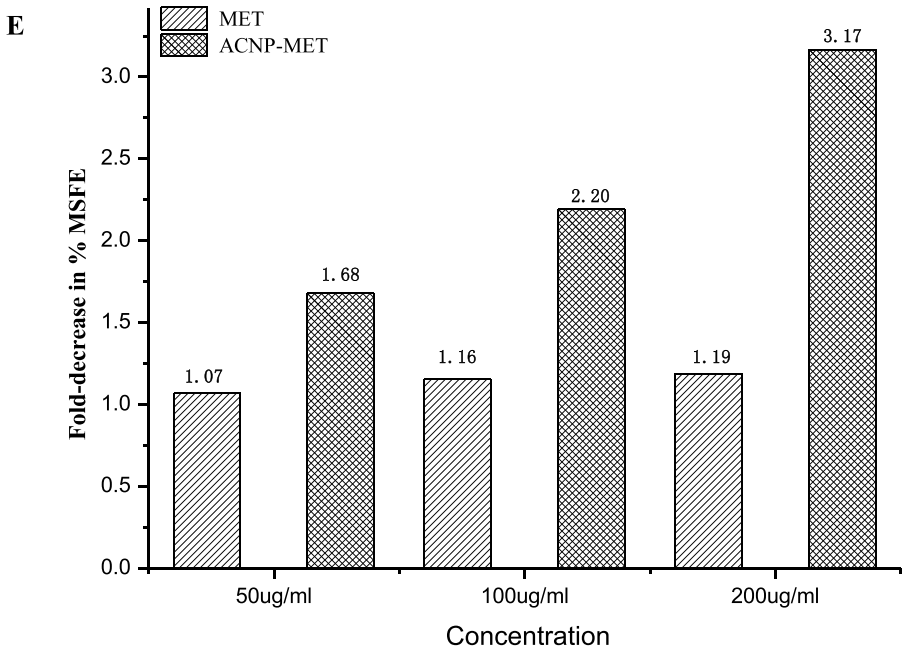

Figure 5 Inhibitory effects of drugs on the self-renewal capacity of hepatocellular CSCs in vitro. (**A**) The CD133 expression of Huh-7 hepatocellular cancer cells after treatment measured by flow cytometry. (**B**) Average percentage of $CD133^+$ cells in Huh-7 hepatocellular cancer cells after treatment. **P*<0.05, ***P*<0.01, statistically significant difference from control; $^{\#}$*P*<0.05, statistically significant difference from MET. ($\bar{x} \pm s$, n=5). (**C**) Representative light microscope images of hepatocellular CSCs growing in sphere medium for 7 days after different treatment (100× magnifications). (**a**) control; (**b**) ACNP 500 μg/mL; (**c**) MET 50 μg/mL; (**d**) ACNP-MET 50 μg/mL; (**e**) MET 100 μg/mL; (**f**) ACNP-MET 100 μg/mL; (**g**) MET 200 μg/mL; (**h**) ACNP-MET 200 μg/mL. (**D**) MSFE of $CD133^+$ cells was calculated as the number of mammospheres (diameter >50 μm) formed in 7 days. **P*<0.05, ***P*<0.01, statistically significant difference from control; $^{\#}$*P*<0.05, $^{\#\#}$*P*<0.01, statistically significant difference from MET. ($\bar{x} \pm s$, n=5). (**E**) Fold-decrease in the MSFE of hepatocellular CSCs mammospheres after different treatment.

ACNP were distributed mainly around or between the hepatocellular CSCs mammospheres and on the surface of the mammospheres rather than evenly in the culture medium (Figure 5C–b). The mammospheres all lived in good condition and there were no significant changes in size and morphology (Figure 5C–b) in comparison with control (Figure 5C–a). Both in MET (Figure 5C–c, e and g) and ACNP-MET (Figure 5C–d, f and h) treated groups, the size and number of mammospheres gradually decreased with the increment of MET concentration. However, the decrement in size and number of mammospheres in ACNP-MET treated groups (Figure 5C–d, f and h) was more significant than that in free MET treated groups (Figure 5C–c, e and g) at the same MET concentration. At 50 μg/mL MET, the mammospheres in ACNP-MET treated group decreased slightly (Figure 5C–c) while there was no observable decrement in free MET treated group (Figure 5C–d). At 100 μg/mL MET, the mammospheres in free MET treated group only decreased slightly without statistical significance (Figure 5C–e) while that in ACNP-MET treated group decreased significantly (Figure 5C–f). At 200 μg/mL MET, the mammospheres almost disappeared in ACNP-MET treated group (Figure 5C–h) while there were still some mammospheres in free MET treated group (Figure 5C–g). In ACNP-MET treated group, the black ACNP-MET particles were distributed mainly around or between the mammospheres and on the surface of mammospheres (Figure 5C–d, f and h), just like the distribution of blank ACNP (Figure 5C–b). These results indicated that ACNP improvement of the effects of MET is dependent on its distribution characteristics.

Figure 5D shows that the MSFE of $CD133^+$ cells was decreasing in a dose-dependent manner when they were cultured in graded concentration of MET and ACNP-MET. It is noteworthy that treatment with 200 μg/mL ACNP-MET completely inhibited the ability of cells to form mammospheres and MSFE in 200 μg/mL ACNP-MET group was 3 times lower than that of 200 μg/mL MET, suggesting that the inhibitive effects of ACNP-MET on the growth of hepatocellular CSCs subpopulations are much stronger than MET (Figure 5E). The analysis of $CD133^+$ cell in tumors demonstrated the same results as that in cultured Huh-7 cells. This result is attractive for overcoming cancer recurrence caused by the presence of this rare cell subpopulation within tumors.

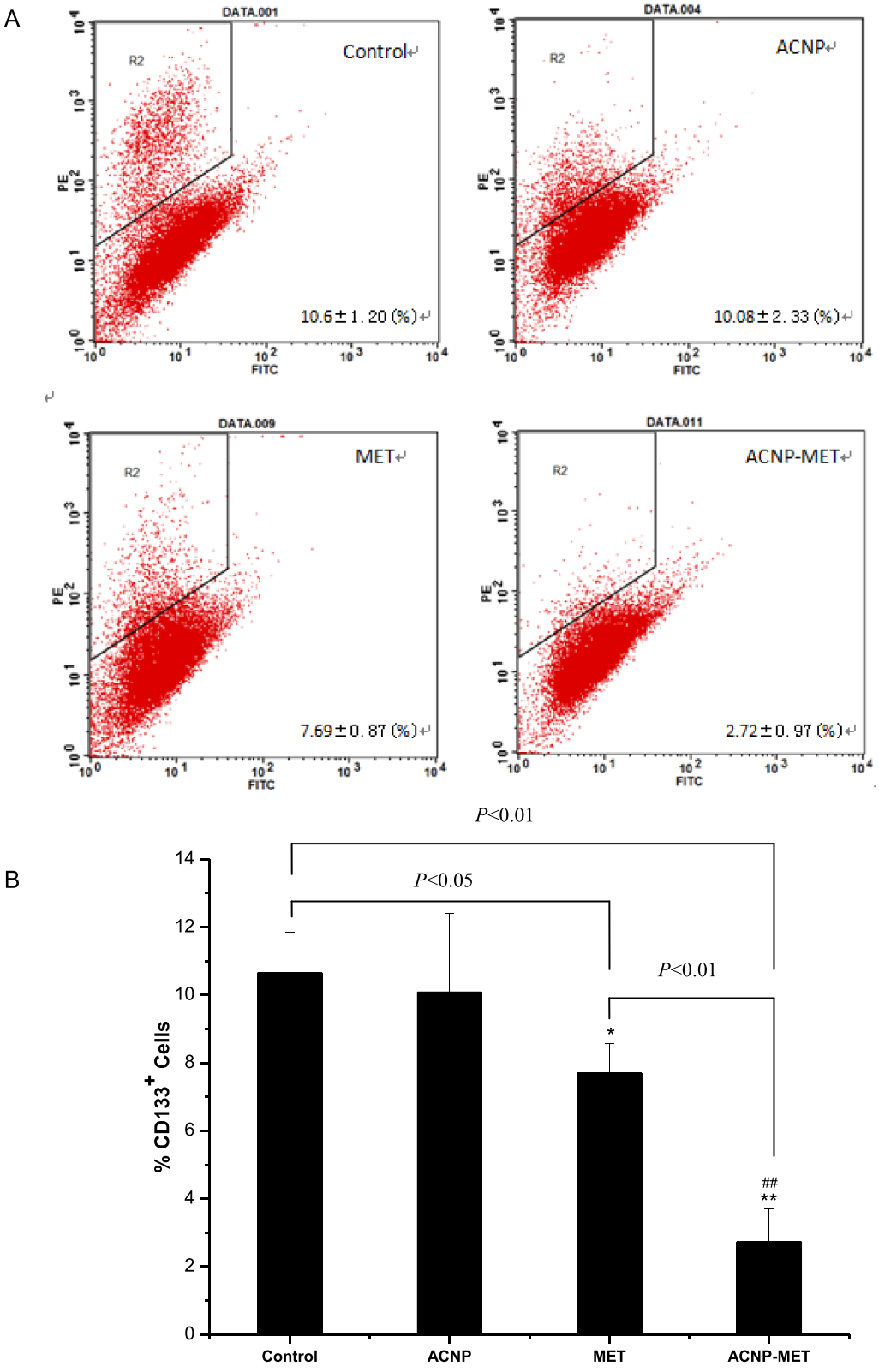

Figure 6 Continued.

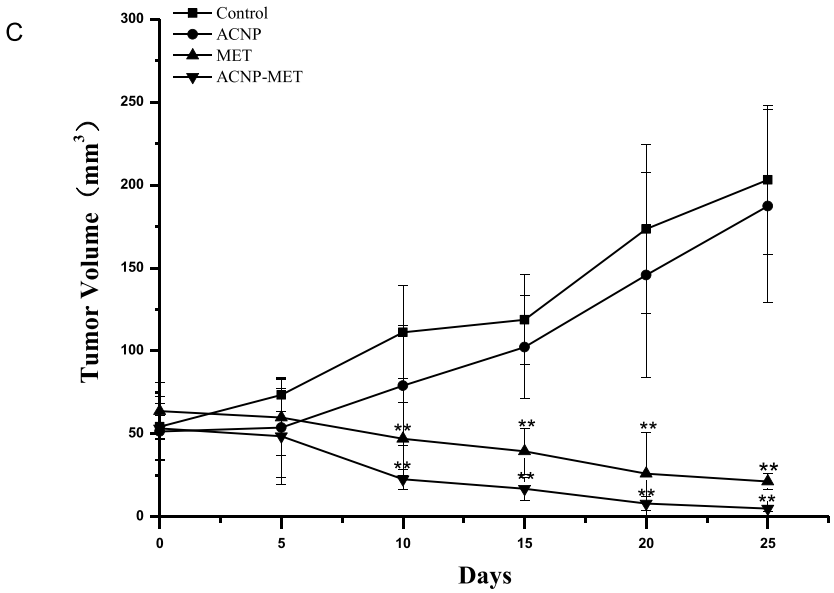

Figure 6 Inhibitory effects of ACNP-MET on the self-renewal capacity of hepatocellular CSCs in vivo. (**A**) Flow cytometry. (**B**) Percentage of CSCs in tumors. (**C**) Tumor volume. Data are shown as mean ± SD, n =6. *P<0.05, **P<0.01, statistically significant difference from control; ##P<0.01, statistically significant difference from MET.

Effects of Drugs on Hepatocellular Cancer Stem Cells (CSCs) in vivo

The hepatocellular cancer cells generated tumors after 3 weeks. It was indicated by the FACS analysis of these tumors that the proportion of $CD133^+$ cells in control tumors was kept at values similar to those in vitro Huh-7 cells (6.08 ± 0.8%). ACNP treated animals had values quite similar to those of normal saline treated animals so we took the values of ACNP as controls in Figure 5A and B. On the 26th day, there was respectively a 1.4- and 3.4-fold reduction of $CD133^+$ cells in tumors treated with MET and ACNP-MET compared with control (Figure 6A and B). These results demonstrated that ACNP-MET could especially inhibit the proliferation of hepatocellular CSCs.

Inhibition of the Growth of Hepatocellular Cancer Stem Cells (CSCs) in vivo

Both MET and ACNP-MET had therapeutic effects on the in vivo human hepatocellular cancer tumor xenografts as shown in Figure 6C. In control animals, the tumors continually grew larger and larger dayly after starting treatment. On the 5th day and 25th day, the tumor volume increased to 73.36 and 203.18 mm^3 respectively from 54.16 mm^3. ACNP treated group showed that there was no significant decrease in tumor growth. On the 5th day and 25th day, the tumor volume increased from 51.45 mm^3 to 53.67 and 187.35 cm^3 respectively with similar growth speed as that of control animals. Both MET and ACNP-MET significantly restricted tumor growth (Figure 6C) but ACNP-MET had stronger effects than MET. In both the MET and ACNP-MET treated animals, the tumor volumes began to decrease. On the 5th day and 25th day, the tumor volumes in the two groups respectively decreased to 21.3 and 4.85 cm^3 from the values at beginning of treatment. Although the tumor volume had similar decreasing curves, the ACNP-MET treated animals had volume growth values smaller than MET at all time points, suggesting the effects of ACNP-MET tended to be stronger than MET.

Considering the MET and ACNP-MET had inhibitive effects on both hepatocellular cancer cells and CSCs, it is believed that the therapeutic effects of MET and ACNP-MET are the sum effects of them on the two kinds of cancer cells. In V_0, the percentage of $CD133^+$ cells (P_{0+}) was 10.6%. In V_I of MET and ACNP-MET treated tumors, the percentage of $CD133^+$ cells (P_{I+}) were 7.69% and 2.72% respectively. On the 26th day, V_0=203.18 mm^3, the volume of $CD133^+$ cells was V_{0+}=21.62 mm^3, the volume of $CD133^-$ cells was V_{0-}=181.56 mm^3. In MET treated tumors, V_I=21.3 mm^3, $V_{I+}=V_IP_{I+}$=0.164 mm^3, $V_{I-}=V_IP_{I-}$=21.136 mm^3, I_V=89.52%. I_{V+}=99.24% and I_{V-}=88.36%. In ACNP-MET treated tumors, V_I=4.85 mm^3, V_{I+}=0.0012 mm^3, V_{I-}=4.8488 mm^3, I_V=97.61%. I_{V+}=99.99%, I_{V-}=97.33%. The ratio of V_I, V_{I+} and V_{I-} of MET treated tumor to those of ACNP-MET treated tumor were respectively 4.39, 136.67 and 4.36, suggesting ACNP-MET's effect on increasing MET's effects on CSCs was far stronger than its effect on increasing MET's effects on CCCs, although the two kinds of effect

were both strong in vivo. From these results, it may be said that I_V is largely equal to I_{V-} rather than I_{V+}, reflecting such a principle: the effects of drugs on tumor size are finally determined by their effects on CCCs.

Discussion

This paper reported the preparation and effects of ACNP-MET on CSCs, hepatocellular Huh-7 cancer cells, and in vivo tumors. MET is used to treat type II diabetes and polycystic ovary syndrome. The landmark evidence for the protective effect of MET in cancer was provided by Evans et al in 2005.[44] Later, several other groups reported that MET could significantly reduce the risk of cancer death in 2013.[45–49] However, there has been scarce literature on the effects of MET on hepatocellular cancers. Our experiment demonstrated that MET is possibly effective in treatment of hepatocellular cancers and the mechanism for the therapeutic effects may be through its inhibitory effects on CSCs and common cancer cells (CCC), while its anti-CSC effects are stronger than its anti-CCC effects. When it was prepared into a nanodrug delivery system (NDDS) with ACNP as carriers (ACNP-MET), the effects of MET on hepatocellular cancer increased significantly, regardless of being in vitro or in vivo.

ACNP are porous particles with a broad absorption spectrum for chemicals. It is easy to put chemical particles such as drugs in the micro holes of ACNP, relying on the adsorption characteristics. ACNP as a cancer drug carrier has special characteristics in the release of the drugs they carry. ACNP adsorb chemical particles generally by physical interactions and no covalent bond needs to form between ACNP and adsorbed matters, so that, the adsorbed drugs can easily disintegrate out from the surface of ACNP again, becoming free drug particles. An outstanding property of ACNP is that the drug concentration around the carriers is in the dynamic balance with the quantity of the drugs loaded on them and can be correctly calculated in mathematical equation, as that obtained from our experiments. Thus, it is very favorable to maintain the drug concentration of local organizations in body through the controlling of drug-loading during preparation.[24] MET belongs to small molecule drug, the relative molecular mass is 165.62. Experiments demonstrated it is easy for MET to be adsorbed in the inside surface of micro pores of ACNP to build ACNP-MET. The adsorption rate between ACNP and MET is relatively high, ie, the adsorption saturation was achieved in 4 hours. The maximum dose for this drug delivery system is 256.17 mg/g. The mass ratio between MET and the ACNP is 1:4. The preparation method is easy and effective.

As shown in Figure 5c, a lot of black particles on the mammospheres are ACNP-MET particles, suggesting ACNP-MET has good affinity to CSCs in liquid environment, ie, ACNP-MET is not evenly precipitated in the bottom of the culture dish but tends to be distributed on the surface of mammospheres and can enter the mammospheres, which provides the best proof for ACNP, as a drug carrier, having tissue targeting effects and it is especially beneficial to use in the killing of cancer cells and organoid cancer cells in body fluid such as in tissue fluid, hydrothorax and ascites. This kind of orientation mechanism of ACNP may be related to the hydrophobic interaction between ACNP and small lipid molecules of cell membranes. At the same time, because ACNP-MET has good drug release properties, there is a dynamic equilibrium between the drug loading and the concentration around ACNP-MET in the drug particles, which results in the drug concentration around CSCs being much higher than that in the nutrient solution, which is quite favorable in the development of drug action on cancer cells. Therefore, compared with the MET group, ACNP-MET had a stronger inhibitory effect on CSCs. It is of significance that ACNP-MET has affinity for CSCs in the physiological solution. For tumor patients, CSCs and cancer cells may exist in various kinds of bodily fluids, such as blood, tissue fluid, lymph, pathological pleural effusion, ascites, joint effusion and local tissue fluid, etc. The affinity of ACNP for CSCs in the fluid is conducive for killing cancer cells in liquid and brings into full play drugs against recurrence and metastasis because the relapse source must exist in body fluid and the metastasis must pass through body fluid.

CD133 is a transmembrane glycoprotein. It has been found that CD133 is expressed in hepatocellular cancer cells and other solid tumor stem cells.[50,51] It has been widely used for sorting and identification of CSCs for many solid tumors.[52,53] In our study, $CD133^+$ cells sorted from Huh-7 cells could proliferate into mammospheres in the serum-free medium. At the same time, when they were enzyme dissociated into single cell suspensions, these primary mammospheres could further generate the secondary. This result indicated that the Huh-7 $CD133^+$ cells possess the characteristics of hepatocellular CSCs.

Previous studies demonstrated that CSCs can escape conventional chemotherapy. Therefore, the drugs with anti-CSC effects may have stronger therapeutic effects on cancers. ACNP-MET has stronger anti-CSC effect than MET so ACNP-MET

has more significant therapeutic effects, as the experiment demonstrated, displaying more promise in clinical use. The quantity and size of mammospheres reflect CSCs' ability of self-renewal and proliferation.[36,39] The self-renewal capacity of CSCs is more powerful and the tumorigenic potential of CSCs is greater. In order to research the effects of drugs on tumorigenic potential of hepatocellular CSCs we performed the formation of mammospheres in culture, as well as in xenograft hepatocellular Huh-7 tumors. Results demonstrated that MET has inhibitory effects on both hepatocellular CSCs and CCCs both in vitro and in vivo. ACNP as carriers in ACNP-MET, significantly increases MET's effects on CSCs and CCCs both in vitro and in vivo.

The in vivo effect of drugs on CSCs resulting in inhibition of tumor volumes seems to be difficult to evaluate, because it is the sum of drug's effects on CSCs and CCCs, and to form a tumor, CSCs must differentiate into CCCs so that the tumor size is in fact mainly the outcome of CCC proliferation. Although the effect of drugs on CSCs can be determined in vitro through cancer cell culture, the quantitative relation between CSC inhibition and tumor size is not clear. To assess the effects of MET and ACNP-MET on CSCs and CCCs in vivo, we had to establish such a method to analyze in vivo effects of drugs on CSCs and CCCs through CSC analysis of tumor. The central idea of the method is that the tumor is composed of CSCs and CCCs without needing to consider the other tissue components. Thus, the tumor volume is separated into two parts, one of which is occupied by CSCs, which is represented by $CD133^+$ cells, and the other is occupied by CCCs, which is represented by $CD133^-$ cells. The volume of CSCs and CCCs in the tumor can easily be calculated from the percentage of CSCs in the tumor, which can easily be obtained through analysis of the tumor. Using this method for analysis, it was found that the inhibition rate of MET and ACNP-MET on tumor volume (I_V) is largely equal to their inhibition rate on CCCs (I_{V-}) rather than their inhibition rate on CSCs (I_{V+}), which is obviously higher than I_V, suggesting the in vivo anti-CSC effect of drugs would be underestimated from I_V. The fact of $I_{V+}>I_V$ for MET and ACNP-MET indicate that the two drugs are more significant in the prevention of tumor relapse and metastasis than in causing the tumor to decrease.

Up until now, there has been a lot of literature on the mechanisms in nanodrug delivery system (NDDS) increasing the therapeutic effects of anticancer drugs,[54–59] of which the most important is NDDS's targeting effects on cancer tissue,[60,61] cells[29,43,61–65] and even special molecules.[32,33,64–66] Because ACNP is biologically inert, it is considered that the ability of ACNP to increase the effects are mainly dependent on its tissue and cell targeting effects. ACNP tended to be distributed around the cancer cells in culture medium and inside the CSC mammospheres, as the in vitro experiments demonstrated, providing reliable proof of its tissue- and cell-targeting effects. In vivo, ACNP, with its tissue targeting, carries MET to tumors and thereby increase the therapeutic effects of MET on tumors. Comparing the effects of ACNP-MET's in vitro and in vivo, it may be found that its in vivo effects are much stronger than its in vitro effects, which may be because its tissue-targeting effect develops a more important role in an animal's body than in cell culture medium.

Conclusion

In this study, we prepared an ACNP-MET drug delivery system and researched its effects on Huh-7 human hepatocellular CSCs. Results demonstrated that both MET and ACNP-MET significantly decreased the fraction of $CD133^+$ cells in Huh-7 human hepatocellular cells and in vivo tumors, but ACNP-MET had more significant effects than MET, as shown by experiments, on the effective of mammosphere formation, the growth of hepatocellular CSC mammosphere, and the volume of tumor. These results not only suggest that nano drug delivery system increased the effects of MET, but also shed light on the mechanisms of the therapeutic effects of MET and ACNP-MET on hepatocellular cancers. They can selectively inhibit Huh-7 hepatocellular CSCs to prevent recurrence and metastasis of hepatocellular cancer in future. ACNP, as a good nano-carrier, could strengthen the effect of MET by carrying drugs to the micro-environment of hepatocellular CSCs. The present study provided a starting point of an effective strategy for the treatment of hepatocellular cancers with potential to improve hepatocellular cancer therapy.

Funding

This work was supported by National Basic Research Program of China (2010CB933904) and Major New Drug Creation Program of China (2011ZX09102-001-15).

Disclosure

The authors report no conflicts of interest in this work.

References

1. Parkin DM, Bray F, Ferlay J, Pisani P. Estimating the world cancer burden: globocan. *Int J Cancer*. 2000;94(2):153–156. doi:10.1002/ijc.1440
2. Hollstein MC, Wild CP, Bleicher F, et al. p53 mutations and aflatoxin B 1 exposure in hepatocellular carcinoma patients from Thailand. *Int J Cancer*. 1993;53:51–55. doi:10.1002/ijc.2910530111
3. Tong CM, Ma S, Guan XY. Biology of hepatic cancer stem cells. *J Gastroenterol Hepatol*. 2011;26:1229–1237. doi:10.1111/j.1440-1746.2011.06762.x
4. Block TM, Mehta AS, Fimmel CJ, Jordan R. Molecular viral oncology of hepatocellular carcinoma. *Oncogene*. 2003;22:5093–5107. doi:10.1038/sj.onc.1206557
5. Song Y-J, Zhang S-S, Guo X-L, et al. Autophagy contributes to the survival of CD133+ liver cancer stem cells in the hypoxic and nutrient-deprived tumor microenvironment. *Cancer Lett*. 2013;339:70–81. doi:10.1016/j.canlet.2013.07.021
6. Gish RG. Hepatocellular carcinoma: overcoming challenges in disease management. *Clin Gastroenterol Hepatol*. 2006;4:252–261. doi:10.1016/j.cgh.2006.01.001
7. Marquardt JU, Factor VM, Thorgeirsson SS. Epigenetic regulation of cancer stem cells in liver cancer: current concepts and clinical implications. *J Hepatol*. 2010;53:568–577. doi:10.1016/j.jhep.2010.05.003
8. Boman BM, Wicha MS. Cancer stem cells: a step toward the cure. *J Clin Oncol*. 2008;26:2795–2799. doi:10.1200/JCO.2008.17.7436
9. Burgos-Ojeda D, Rueda BR, Buckanovich RJ. Ovarian cancer stem cell markers: prognostic and therapeutic implications. *Cancer Lett*. 2012;322:1–7. doi:10.1016/j.canlet.2012.02.002
10. Lobo NA, Shimono Y, Qian D, Clarke MF. The biology of cancer stem cells. *Annu Rev Cell Dev Biol*. 2007;23:675–699. doi:10.1146/annurev.cellbio.22.010305.104154
11. Ma S, Lee TK, Zheng BJ, Chan KW, Guan XY. CD133+ HCC cancer stem cells confer chemoresistance by preferential expression of the Akt/PKB survival pathway. *Oncogene*. 2008;27:1749–1758. doi:10.1038/sj.onc.1210811
12. Ma S, Chan KW, Hu L, et al. Identification and characterization of tumorigenic liver cancer stem/progenitor cells. *Gastroenterology*. 2007;132:2542–2556. doi:10.1053/j.gastro.2007.04.025
13. Suetsugu A, Nagaki M, Aoki H, Motohashi T, Kunisada T, Moriwaki H. Characterization of CD133+ hepatocellular carcinoma cells as cancer stem/progenitor cells. *Biochem Biophys Res Commun*. 2006;351:820–824. doi:10.1016/j.bbrc.2006.10.128
14. Stephanie M. Biology and clinical implications of CD133+liver cancer stem cells. *Exp Cell Res*. 2013;319:126–132. doi:10.1016/j.yexcr.2012.09.007
15. Dowling R, Goodwin P, Stambolic V. Understanding the benefit of metformin use in cancer treatment. *BMC Med*. 2011;9:33. doi:10.1186/1741-7015-9-33
16. Yang Q, Zhang T, Wang C, Jiao J, Li J, Deng Y. Coencapsulation of epirubicin and metformin in PEGylated liposomes inhibits the recurrence of murine sarcoma S180 existing $CD133^{+}$cancer stem-like cells. *Eur J Pharma Biopharmaceut*. 2014;88:737–745. doi:10.1016/j.ejpb.2014.10.006
17. Zhang P, Li H, Tan X, Chen L, Wang S. Association of metformin use with cancer incidence and mortality: a meta-analysis. *Cancer Epidemiol*. 2013;37:207–218. doi:10.1016/j.canep.2012.12.009
18. Hirsch HA, Iliopoulos D, Tsichlis PN, Struhl K. Metformin selectively targets cancer stem cells, and acts together with chemotherapy to block tumor growth and prolong remission. *Cancer Res*. 2009;69:7507–7511. doi:10.1158/0008-5472.CAN-09-2994
19. Vazquez-Martin A, Oliveras-Ferraros C, Barco SD, et al. The anti-diabetic drug metformin suppresses self-renewal and proliferation of trastuzumab-resistant tumor-initiating breast cancer stem cells. *Menendez Breast Cancer Res Treat*. 2011;126:355–364. doi:10.1007/s10549-010-0924-x
20. Vazquez-Martin A, Oliveras-Ferraros C, Cu Fi S, Del Barco S, Martin-Ca Stillo B, Menendez JA. Metformin regulates breast cancer stem cell ontogeny by transcriptional regulation of the epithelial–mesenchymal transition (EMT) status. *Cell Cycle*. 2010;9:3807–3814. doi:10.4161/cc.9.18.13131
21. Bao B, Wang Z, Ali S, et al. Metformin inhibits cell proliferation, migration and invasion by attenuating CSC function mediated by deregulating miRNAs in pancreatic cancer cells. *Cancer Prev Res*. 2012;5:355–364. doi:10.1158/1940-6207.CAPR-11-0299
22. Qiu-Lian Q, Ying-Ge Z. Effects of activated carbon nanoparticles on human gastric carcinoma cell line BGC-823 *in vitro*. *Military Med Sci*. 2009;33(1):29–32.
23. Peng F. *The Mode of Cross-Membrane Transferring and Biological Effects of Nanoparticles* Doctoral dissertation. Zhengzhou University; 2011:27–36.
24. Sun L, Cai Y, Liu Y, Song D, Liu, Y, Yao H, Zhang Y. Activated carbon nanoparticles as carriers of anticancer drugs. *Nano Biomed Eng*. 2013;5(2):94–101.
25. Yang Z, Zhao JX, Li PF, Zhang YG. Effects of activated carbon nanoparticles on anti cancer effect of 5-Fu. *Bull Acad Mil Med Sci*. 2009;33(5):416–420.
26. Zhang H, Sun L, Zhang YG. Intraperitoneal chemotherapy with mitomycin C bound to activated carbon nanoparticles using bioluminescence imaging technology. *Mil Med Sci*. 2011;35(4):299–302.
27. Qu QL, Zhang YG, Yang LZ, Sun L. Intraperitoneal chemotherapy with mitomycin C bound to activated carbon nanoparticles for nude mice bearing human gastric carcinoma. *Zhonghua Zhong Liu Za Zhi*. 2006;28(4):257–260. Chinese.
28. Zhong Y, Shuzheng M, Yingge Z. Using activated carbon nanoparticles to decrease the genotoxicity and teratogenicity of anticancer therapeutic agents. *J Nanosci Nanotechnol*. 2010;10(12):8603–8609.
29. Jiang S, Wang X, Zhang Z, et al. CD20 monoclonal antibody targeted nanoscale drug delivery system for doxorubicin chemotherapy: an *in vitro* study of cell lysis of CD20-positive Raji cells. *Int J Nanomedicine*. 2016;(11):5505–5518. doi:10.2147/IJN.S115428
30. Jumelle C, Mauclair C, Houzet J, et al. Delivery of macromolecules into the endothelium of whole ex vivo human cornea by femtosecond laser-activated carbon nanoparticles. *Br J Ophthalmol*. 2016;100(8):1151–1156. doi:10.1136/bjophthalmol-2015-307610
31. Xie J, Yong Y, Dong X, et al. Therapeutic nanoparticles based on curcumin and bamboo charcoal nanoparticles for chemo-photothermal synergistic treatment of cancer and radioprotection of normal cells. *ACS Appl Mater Interfaces*. 2017;9(16):14281–14291. doi:10.1021/acsami.7b02622

32. Yao HJ, Sun L, Liu Y, et al. Monodistearoylphosphatidylethanolamine-hyaluronic acid functionalization of single-walled carbon nanotubes for targeting intracellular drug delivery to overcome multidrug resistance of cancer cells. *Carbon*. 2016;96:362–376. doi:10.1016/j.carbon.2015.09.037
33. Yao H, Sun L, Li J, et al. A novel therapeutic siRNA nanoparticle designed for dual-targeting CD44 and Gli1 of gastric cancer stem cells. *Int J Nanomedicine*. 2020;15:7013–7034. doi:10.2147/IJN.S260163
34. Chen H, Luo Z, Dong L, et al. CD133/prominin-1-mediated autophagy and glucose uptake beneficial for hepatoma cell survival. *PLoS One*. 2013;8:e56878. doi:10.1371/journal.pone.0056878
35. Dontu G, Abdallah WM, Foley JM, et al. *In vitro* propagation and transcriptional profiling of human mammary stem/progenitor cells. *Genes Dev*. 2003;17:1253–1270. doi:10.1101/gad.1061803
36. Dontu G, Jackson KW, McNicholas E, et al. Role of Notch signaling in cell-fate determination of human mammary stem/progenitor cells. *Breast Cancer Res*. 2004;6:605–615. doi:10.1186/bcr920
37. Eyre R, Alférez DG, Spence K, et al. Patient-derived mammosphere and xenograft tumour initiation correlates with progression to metastasis. *J Mammary Gland Biol Neoplasia*. 2016;21(3–4):99–109. doi:10.1007/s10911-016-9361-8
38. Mariya S, Dewi FN, Suparto IH, et al. Mammosphere culture of mammary cells from cynomolgus macaques (Macaca fascicularis). *Comp Med*. 2019;69(2):144–150. doi:10.30802/AALAS-CM-18-000030
39. Liu J, Li M, Song B, et al. Metformin inhibits renal cell carcinoma in vitro and in vivo xenograft. *Urol Oncol*. 2013;31:264–270. doi:10.1016/j.urolonc.2011.01.003
40. Zhang X, Li F, Zheng Y, et al. Propofol reduced mammosphere formation of breast cancer stem cells via PD-L1/Nanog in vitro. *Oxid Med Cell Longev*. 2019;2019:9078209. doi:10.1155/2019/9078209
41. Klopp AH, Lacerda L, Gupta A, et al. Mesenchymal stem cells promote mammosphere formation and decrease E-cadherin in normal and malignant breast cells. *PLoS One*. 2010;5(8):e12180. doi:10.1371/journal.pone.0012180
42. Silva IA, Bai S, McLean K, et al. Aldehyde dehydrogenase in combination with CD133 defines angiogenic ovarian cancer stem cells that portend poor patient survival. *Cancer Res*. 2011;71:3991–4001. doi:10.1158/0008-5472.CAN-10-3175
43. Yao H-J, Zhang Y-G, Sun L, Liu Y. The effect of hyaluronic acid functionalize d carbon nanotubes loaded with salinomycin on gastric cancer stem cells. *Biomaterials*. 2014;35:9208–9223. doi:10.1016/j.biomaterials.2014.07.033
44. Evans JMM, Donnelly LA, Emslie-Smith AM, Alessi DR, Morris AD. Metformin and reduced risk of cancer in diabetic patients. *Br Med J*. 2005;530:1304–1305. doi:10.1136/bmj.38415.708634.F7
45. Bowker SL, Majumdar SR, Veugelers P, Johnson JA. Increased cancer-related mortality for patients with type 2 diabetes who use sulfonylureas or insulin. *Diabetes Care*. 2006;29:254–258. doi:10.2337/diacare.29.02.06.dc05-1558
46. Libby G, Donnelly LA, Donnan PT, Alessi DR, Morris AD, Evans JMM. New users of metformin are at low risk of incident cancer: a cohort study among people with type 2 diabetes. *Diabetes Care*. 2009;32:1620–1625. doi:10.2337/dc08-2175
47. Landman GW, Kleefstra N, van Hateren KJJ, Groenier KH, Gans RO, Bilo HJ. Metformin associated with lower cancer mortality in type 2 diabetes: ZODIAC-16. *Diabetes Care*. 2010;33:322–326. doi:10.2337/dc09-1380
48. Franciosi M, Lucisano G, Lapice E, Strippoli GF, Pellegrini F, Nicolucci A. Metformin therapy and risk of can- cer in patients with type 2 diabetes: systematic review. *PLoS One*. 2013;8:e71583. doi:10.1371/journal.pone.0071583
49. Decensi A, Puntoni M, Goodwin P, et al. Metformin and cancer risk in diabetic patients: a systematic review and meta-analysis. *Cancer Prev Res*. 2010;3:1451–1461. doi:10.1158/1940-6207.CAPR-10-0157
50. Miraglia S, Godfrey W, Yin AH, et al. A novel five-transmembrane hematopoietic stem cell antigen: isolation, characterization, and molecular cloning. *Blood*. 1997;90:5013–5021. doi:10.1182/blood.V90.12.5013
51. Yin AH, Miraglia S, Zanjani ED, et al. AC133, a novel marker for human hematopoietic stem and progenitor cells. *Blood*. 1997;90:5002–5012. doi:10.1182/blood.V90.12.5002
52. Wu Y, Wu PY. CD133 as a marker for cancer stem cells: progresses and concerns. *Stem Cells Dev*. 2009;18:1127–1134. doi:10.1089/scd.2008.0338
53. Missol-Kolka E, Karbanova J, Janich P, et al. Prominin-1 (CD133) is not restricted to stem cells located in the basal compartment of murine and human prostate. *Prostate*. 2011;71:254–267. doi:10.1002/pros.21239
54. Zhou F, Teng F, Deng P, Meng N, Song Z, Feng R. Recent progress of nano-drug delivery system for liver cancer treatment. *Anticancer Agents Med Chem*. 2018;17(14):1884–1897. doi:10.2174/1871520617666170713151149
55. Huang P, Wang X, Liang X, et al. Nano-, micro-, and macroscale drug delivery systems for cancer immunotherapy. *Acta Biomater*. 2019;85:1–26. doi:10.1016/j.actbio.2018.12.028
56. Fang Z, Pan S, Gao P, et al. Stimuli-responsive charge-reversal nano drug delivery system: the promising targeted carriers for tumor therapy. *Int J Pharm*. 2020;575:118841. doi:10.1016/j.ijpharm.2019.118841
57. Ashfaq UA, Riaz M, Yasmeen E, Yousaf MZ. Recent advances in nanoparticle-based targeted drug-delivery systems against cancer and role of tumor microenvironment. *Crit Rev Ther Drug Carrier Syst*. 2017;34(4):317–353. doi:10.1615/CritRevTherDrugCarrierSyst.2017017845
58. Xue J, Li R, Gao D, Chen F, Xie H. CXCL12/CXCR4 axis-targeted dual-functional nano-drug delivery system against ovarian cancer. *Int J Nanomedicine*. 2020;15:5701–5718. doi:10.2147/IJN.S257527
59. Mi X, Hu M, Dong M, et al. Folic acid decorated zeolitic imidazolate framework (ZIF-8) loaded with baicalin as a nano-drug delivery system for breast cancer therapy. *Int J Nanomedicine*. 2021;16:8337–8352. doi:10.2147/IJN.S340764
60. Yang X, Chen S, Liu X, Yu M, Liu X. Drug delivery based on nanotechnology for target bone disease. *Curr Drug Deliv*. 2019;16(9):782–792. doi:10.2174/1567201816666190917123948
61. Mokhtarzadeh A, Hassanpour S, Vahid ZF, et al. Nano-delivery system targeting to cancer stem cell cluster of differentiation biomarkers. *J Control Release*. 2017;266:166–186. doi:10.1016/j.jconrel.2017.09.028
62. Liu B, Yang W, Che C, et al. Drug delivery system of AS1411 functionalized graphene oxide based composites. *Chem Open*. 2021;10(4):408–413. doi:10.1002/open.202000226
63. Liu Y, Pu Y, Sun L, et al. Folic acid functionalized γ-Cyclodextrin C60, a novel vehicle for tumor-targeted drug delivery. *J Biomed Nanotechnol*. 2016;12:1393–1403. doi:10.1166/jbn.2016.2275
64. Wu HH, Zhou Y, Tabata Y, Gao JQ. Mesenchymal stem cell-based drug delivery strategy: from cells to biomimetic. *J Control Release*. 2019;294:102–113. doi:10.1016/j.jconrel.2018.12.019

65. Jain P, Kathuria H, Momin M. Clinical therapies and nano drug delivery systems for urinary bladder cancer. *Pharmacol Ther*. 2021;226:107871. doi:10.1016/j.pharmthera.2021.107871
66. Yu H, Jin F, Liu D, et al. ROS-responsive nano-drug delivery system combining mitochondria-targeting ceria nanoparticles with atorvastatin for acute kidney injury. *Theranostics*. 2020;10(5):2342–2357. doi:10.7150/thno.40395